International Journal of Thermophysics, Vol. 18, No. 5, 1997

Viscosities of Molten Alkali–Metal Bromides and Iodides

Y. Sato,[1,2] M. Fukasawa,[3] and T. Yamamura[1]

Received February 5, 1997

Viscosities of molten alkali–metal bromides and iodides, whose reported values are scattered, have been measured by the use of a capillary viscometer made of quartz which is newly designed to obtain a high precision. The viscometer consists of the quartz capillary with a funnel of the suspended level type, and the melt is sealed in it under vacuum. The total error in the measurement is estimated to be within 0.7% at high temperatures. Viscosities of all the alkali–metal bromides and iodides show similar values at a constant temperature. Viscous flow behaviors of all the alkali–metal halides are discussed based on the activation energy and the hard sphere model. The apparent activation energy increases with an increase in the melting temperature of the salt. The viscosity of the alkali–metal halide melt at the melting temperature increases as the ratio of hard sphere volume to hole volume calculated from the surface tension.

KEY WORDS: alkali halide; bromide; capillary viscometer; iodide; molten salt; viscosity; viscous flow.

1. INTRODUCTION

Viscosity is very important thermophysical property not only of molten salts but of all liquids. In the case of molten salts, however, there are not enough publications and big discrepancies are frequently found among the values reported due to the difficulties of measuring the viscosity precisely at high temperatures. Although the oscillating viscometer or rotating viscometry is popular for high-temperature melts, the present authors have found that a classical method, the capillary viscometry, was a better

[1] Department of Metallurgy, Tohoku University, Sendai 980-77, Japan.
[2] To whom correspondence should be addressed.
[3] Sumitomo Mining, Tokyo 105, Japan.

0195-928X/97/0900-1123$12.50/0

candidate for hygroscopic or unstable molten salts by improving the viscometer to adapt to high temperature.

A capillary viscometer made of quartz was designed and constructed, and the viscosity of molten alkali halides was precisely measured up to 1200 K. The factors affecting viscous flow of alkali halides were studied based on the viscosity measured. It was found that the activation energy of viscous flow is related to the melting temperature, and the logarithmic viscosity at melting temperature is also related to the ratio of hard sphere volume to hole volume in the melt.

2. EXPERIMENTAL PROCEDURE

2.1. Apparatus

In the vertical type of capillary viscometer, viscosity, η, is expressed by the well-known Hagen–Poiseuilles equation:

$$\eta = \frac{\pi r^4 \rho g h}{8(L+nr)\,V} t - \frac{m\rho V}{8\pi(L+nr)} \frac{1}{t} \tag{1}$$

where, ρ is the density of the liquid, r and L are the radius and length of the capillary, h is the effective height of the liquid column, V is the volume of the timing bulb, g is the gravitational acceleration, t is the time interval for the flow of liquid, and m and n are constants. For a given viscometer, the coefficients of right-hand terms in Eq. (1) except t and ρ are constant, therefore Eq. (1) is rewritten by introducing the kinematic viscosity, ν.

$$\nu = \eta/\rho = C_1 t - C_2/t \tag{2}$$

Currently, there are many problems in the capillary viscometer at high temperatures, although it is the most reliable and precise method and is widely accepted at room temperature. The problems are the difficulties, for example, in getting the capillary, with a fine and uniform bore made of refractory materials such as quartz, to feed a constant amount of the liquid, to heat the viscometer uniformly, and to detect the liquid meniscus. Although some investigators used the capillary viscometer for molten salts, most of their apparatuses [1–6] included electrical probes or the melt was not completely sealed in it. In those cases of viscometers, either wetting and detaching the liquid surface by the electrical probe cause the uncertainty or the fact that the melt may be affected by the atmosphere.

In this work, a newly designed capillary viscometer for high temperatures has been realized by using a transparent electric furnace, the Gold

Furnace [7]. Essential parameters in this work for designing the viscometer are as follows: (a) the meniscus is detected visually, (b) the lower end of the capillary does not touch the bulk liquid for removing the effect of the volume change of the liquid, (c) the Reynolds number in the capillary is less than 100 to maintain the stable layer flow, (d) the range of kinematic viscosity of the liquid is $(0.3\text{–}1.7) \times 10^{-6}\ m^2 \cdot s^{-1}$, which are the values of pure water for the calibration at temperatures between 274 and 354 K, (e) the flow time is between 100 and 400 s, and (f) salts must be sealed completely in the viscometer under vacuum to prevent the salt from exposition to air. Figure 1 shows the viscometer with the filtration chamber used in this work. The inner diameter and the length of the capillary, typically 0.4 and 80 mm, are determined by considering the above requirements. The viscometer, made entirely of quartz, has a funnel with a small hole, a timing bulb, and a capillary tube. The capacity of the timing bulb is about 4 ml. The funnel accepts an excess volume of the liquid for the timing bulb. For repeating measurements, the liquid is moved from the bottom to the funnel through the hole by reversing the viscometer. The upper and lower fiducial marks are at both ends of the timing bulb, where the inner diameters are 3–4 mm. For this type of viscometer, the surface

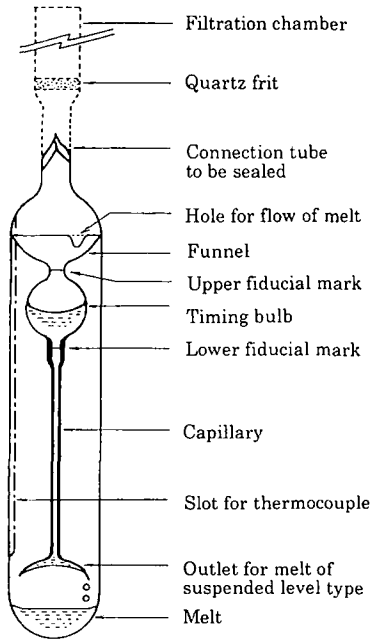

Fig. 1. The capillary viscometer made of quartz.

tension of the liquid affects the measurement. The force, F, is generated vertically on the curved surface by the surface tension of the liquid. The force on the surface with a curvature radius, a_s, is expressed using the surface tension, γ, as $F = 2\gamma/a_s$. As shown in Fig. 2a, the force F_1 acting on the surface in the timing bulb is directed upward, and the force F_2 acting on the surface at the free end of the capillary is also directed upward. The forces change the effective height, h, in Eq. (1). Additional effective height caused by surface tension, Δh, is expressed as $\Delta h = 2\gamma/\rho g a_s$. Δh affects the measurement unless Δh for both the sample salts and the water is the same. If the a_s of the meniscus is assumed to be equal to the radius of timing bulb (6 mm), Δh is 1.44 and 2.45 mm for molten NaBr at 1100 K ($\gamma = 95.85$ mN $\cdot$ m^{-1}) and water at 298 K, respectively. However, the real a_s is several times larger than 6 mm for most of the time of flow, and the difference between both Δh values is less than the above value.

As mentioned above, the difference between the Δh for sample salts and water in the timing bulb is very small compared with the length of the capillary. However, Δh caused by F_2 at the free end of the capillary remains. If a normal cut end is used, F_2 is relatively large as shown in Fig. 2a, therefore a downward funnel was built at the end of the capillary to resolve the problem as shown in Fig. 2b. The downward funnel is wetted by the liquid and makes a concave curvature of the liquid surface in it. The direction of the force caused in the downward funnel is opposite to the

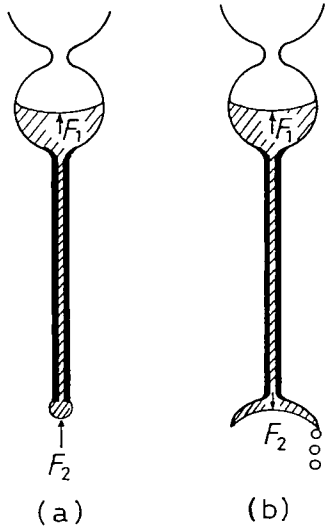

Fig. 2. Forces caused vertically by surface tension at the liquid surface.

force caused in the timing bulb, and the error caused by surface tension is minimized.

Prior to the measurement, the sample salt is fed into the filtration chamber under vacuum. Then it is melted and filtrated in a conventional furnace, and the filtration chamber is sealed off from the viscometer. Figure 3 shows the whole apparatus for viscosity measurement. The viscometer is set in the transparent Gold Furnace, in which the temperature uniformity is kept within 0.5 K around the viscometer. The steel frame with the furnace can be rotated 180° in order to let the liquid move from the bottom to the funnel through the hole for repeating the measurement. The interval between the times in which the meniscus passes through the upper and the lower fiducial marks is determined visually from the outside of the furnace using a digital stopwatch with a precision of 0.01 s. This procedure is repeated three to five times at the same temperature, and the reproducibility of the time measurement is within 0.2 s, which corresponds to 0.05–0.2% of the flow time.

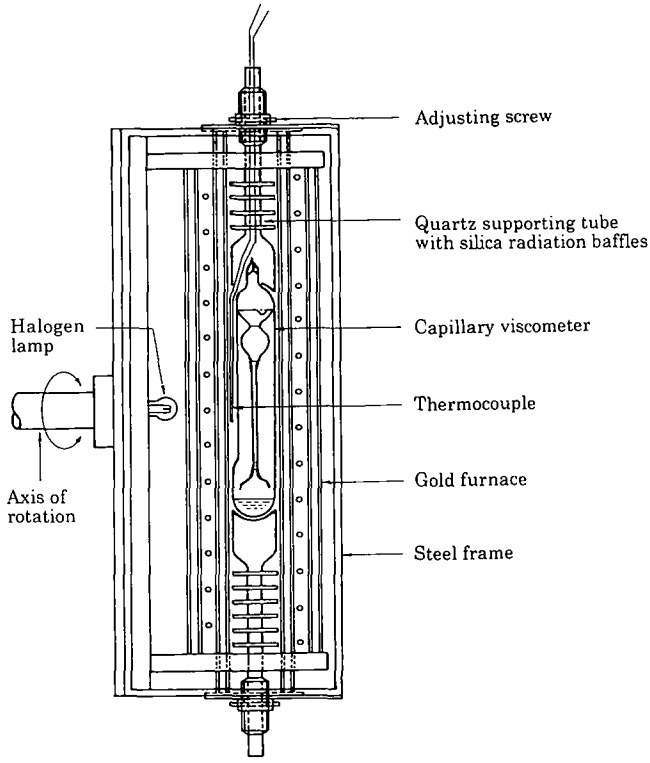

Fig. 3. View of the entire apparatus for viscosity measurement.

All the chemicals used are reagent grade and purified as described in a previous paper [7].

2.2. Determination of the Viscometer Constants

In general, C_2/t is small compared with $C_1 t$ in Eq. (2), for example, the ratio is less than 2% when t is 150 s in this work. In this work, water was used as the calibration liquid for determining the constants, C_1 and C_2, for the following reasons: (a) the viscosity and density of water are most precisely known and most reliable compared with those of all other liquids, molten salts, electrolyte aqueous solution, organic liquids, etc.; (b) water covers a wide range of kinematic viscosity which is nearly the same as that of molten alkali–metal halides; (c) water has a higher surface tension than other room-temperature liquids, so the error caused by surface tension is lowered; (d) no electrical conductivity is required for the calibration liquid because the meniscus is observed visually, not by using electrical probes; and (e) the difference between the viscometer constant at room temperature and that at high temperature is negligible using quartz.

For determination of the viscometer constants, pure water is sealed into the viscometer under vacuum and the flow times are measured in a water thermostat at 10 temperatures between 274 and 348 K. The constants are calculated using the least-squares method through the flow time measured. The temperature of the thermostat is kept within ± 0.05 K. The constants are measured before and after the measurement of molten salts to check the corrosion of the capillary.

3. RESULTS AND DISCUSSION

Table I shows the kinematic viscosities measured directly and the viscosities calculated using the density data reported by Yaffe et al. [8]. Viscosities are shown in Figs. 4 to 13 with literature values [9–15]. The present results show a good Arrhenian relationship. Table II shows the regression equations obtained by the least-squares method.

The factors which cause the errors in this measurement have been examined as follows.

(a) Expansion and slant of the capillary: Although the difference between room temperature and the working temperature reaches 900 K, the dimensional consideration of Eq. (1) and the expansion coefficient of quartz ($5.7 \times 10^{-7}\ K^{-1}$) give an error only 0.04% of C_1 in Eq. (2) even at the highest temperature. The error caused by the slant of the viscometer is less than 0.06% assuming a slant of less than 2°.

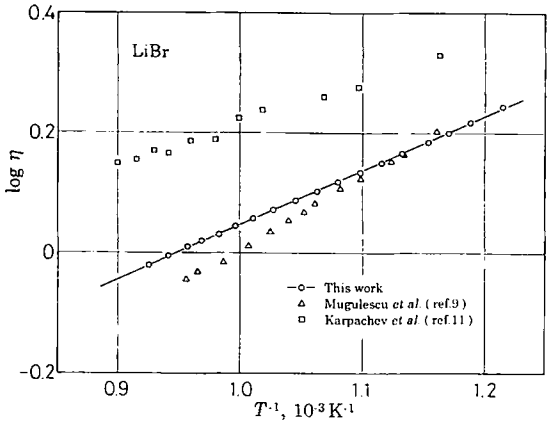

Fig. 4. Viscosity (in mPa·s) of molten lithium bromide.

(b) Drainage of the melt: Jones and Stauffer [16] reported that drainage was proportional to the term, v/t. The term is nearly the same as C_1 in Eq. (2) and is almost independent of the sample salt using an identical viscometer. Indeed the drainage is considered to be very small for molten alkali–metal halides, with their low viscosities, and is found to be negligible by visual observation.

(c) Surface tension of the liquid: When the surface tension of the melt is different from the calibration liquid, water, the effective height of the liquid column may be different; thus the viscometer is designed to minimize the effect of surface tension as mentioned above. For each of F_1 and F_2 in

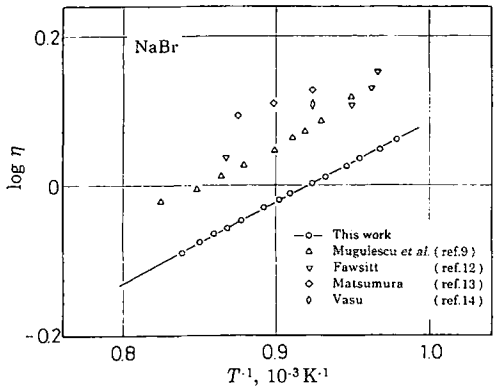

Fig. 5. Viscosity (in mPa·s) of molten sodium bromide.

Table I. Kinematic Viscosities and Viscosities of Molten Alkali Metal Bromides and Iodides

	T (K)	ν (10^{-6} m^2·s^{-1})	η (mPa·s)
LiBr	823.3	0.6933	1.7535
	841.2	0.6555	1.6502
	854.7	0.6319	1.5853
	867.1	0.6131	1.5330
	883.7	0.5895	1.4677
	896.4	0.5715	1.4182
	911.0	0.5532	1.3674
	926.2	0.5346	1.3161
	941.4	0.5167	1.2671
	957.0	0.5013	1.2242
	973.9	0.4859	1.1811
	989.8	0.4716	1.1415
	1003.8	0.4596	1.1084
	1018.0	0.4478	1.0756
	1032.7	0.4379	1.0476
	1045.5	0.4284	1.0214
	1062.4	0.4169	0.9894
	1081.7	0.4044	0.9547
NaBr	1022.0	0.4922	1.1517
	1033.8	0.4784	1.1149
	1048.1	0.4688	1.0870
	1057.1	0.4591	1.0612
	1072.9	0.4460	1.0250
	1083.2	0.4390	1.0054
	1100.0	0.4270	0.9719
	1108.7	0.4207	0.9547
	1121.4	0.4128	0.9324
	1139.9	0.3998	0.8971
	1152.2	0.3925	0.8767
	1163.9	0.3855	0.8575
	1176.2	0.3787	0.8384
	1192.2	0.3699	0.8142
KBr	1010.8	0.5714	1.2139
	1021.4	0.5571	1.1787
	1032.8	0.5433	1.1445
	1043.7	0.5302	1.1120
	1054.8	0.5157	1.0770
	1062.9	0.5079	1.0572
	1073.5	0.4977	1.0316
	1084.1	0.4873	1.0058
	1092.4	0.4787	0.9848

Table I. *(Continued)*

	T (K)	ν ($10^{-6}\ m^2 \cdot s^{-1}$)	η (mPa · s)
	1099.9	0.4721	0.9684
	1114.9	0.4597	0.9371
	1124.0	0.4503	0.9147
	1135.9	0.4411	0.8917
	1144.3	0.4345	0.8752
	1154.4	0.4264	0.8554
	1165.8	0.4184	0.8355
	1174.7	0.4126	0.8208
	1184.9	0.4061	0.8045
	1194.0	0.4005	0.7904
RbBr	971.4	0.5530	1.4920
	982.5	0.5365	1.4409
	1012.3	0.4983	1.3225
	1027.1	0.4816	1.2706
	1043.2	0.4643	1.2169
	1056.6	0.4508	1.1751
	1074.9	0.4335	1.1215
	1104.0	0.4099	1.0475
	1119.0	0.3994	1.0144
	1136.0	0.3884	0.9792
	1149.7	0.3782	0.9480
	1165.2	0.3690	0.9188
	1196.8	0.3491	0.8574
CsBr	911.8	0.5589	1.7494
	930.5	0.5283	1.6414
	951.6	0.4978	1.5340
	975.7	0.4672	1.4258
	992.2	0.4484	1.3594
	1013.1	0.4278	1.2861
	1032.3	0.4089	1.2195
	1050.2	0.3939	1.1663
	1074.8	0.3749	1.0986
	1092.9	0.3631	1.0562
	1113.4	0.3505	1.0105
	1132.4	0.3373	0.9646
	1153.3	0.3261	0.9243
	1171.9	0.3175	0.8927
	1191.6	0.3076	0.8575
LiI	742.3	0.6812	2.1179
	758.9	0.6439	1.9921

Table I. *(Continued)*

	T (K)	ν (10^{-6} m$^2 \cdot$ s^{-1})	η (mPa $\cdot$ s)
	771.1	0.6188	1.9074
	785.1	0.5901	1.8115
	802.8	0.5599	1.7095
	824.4	0.5266	1.5975
	836.2	0.5096	1.5402
	851.2	0.4899	1.4741
	864.4	0.4737	1.4195
	879.1	0.4570	1.3633
	892.5	0.4435	1.3177
	908.3	0.4277	1.2644
	923.5	0.4138	1.2175
	936.4	0.4028	1.1805
	949.9	0.3927	1.1461
	966.5	0.3788	1.0997
	981.4	0.3683	1.0642
	997.7	0.3588	1.0313
	1011.8	0.3493	0.9996
	1028.3	0.3390	0.9648
NaI	940.6	0.4179	1.1429
	950.8	0.4088	1.1139
	964.3	0.3990	1.0821
	972.8	0.3923	1.0608
	983.2	0.3802	1.0244
	993.4	0.3724	0.9999
	1003.0	0.3650	0.9767
	1013.2	0.3589	0.9569
	1024.2	0.3522	0.9353
	1031.5	0.3472	0.9196
	1042.4	0.3408	0.8990
	1053.0	0.3352	0.8809
	1064.9	0.3278	0.8579
	1073.2	0.3251	0.8481
	1082.9	0.3193	0.8302
	1093.6	0.3135	0.8117
	1103.6	0.3095	0.7985
	1116.5	0.3031	0.7783
KI	965.2	0.5439	1.3255
	985.4	0.5158	1.2470
	997.9	0.5035	1.2113
	1013.4	0.4878	1.1664
	1027.4	0.4749	1.1292

Table I. *(Continued)*

	T (K)	ν (10^{-6} m$^2 \cdot$ s^{-1})	η (mPa $\cdot$ s)
	1041.1	0.4622	1.0928
	1058.3	0.4491	1.0545
	1075.4	0.4357	1.0159
	1091.9	0.4250	0.9843
	1101.6	0.4185	0.9654
	1119.7	0.4060	0.9294
	1134.5	0.3957	0.9003
	1147.4	0.3876	0.8770
	1162.9	0.3783	0.8505
	1177.3	0.3725	0.8322
	1193.0	0.3652	0.8104
RbI	933.7	0.5187	1.4947
	954.9	0.4897	1.3994
	977.7	0.4611	1.3057
	996.3	0.4411	1.2396
	1014.7	0.4240	1.1825
	1032.9	0.4051	1.1214
	1055.3	0.3852	1.0564
	1073.7	0.3708	1.0092
	1095.5	0.3562	0.9606
	1115.9	0.3440	0.9197
	1134.3	0.3323	0.8815
	1153.3	0.3229	0.8493
	1172.0	0.3133	0.8174
	1193.6	0.3030	0.7830
CsI	916.8	0.4804	1.5164
	936.5	0.4537	1.4214
	954.5	0.4346	1.3523
	975.1	0.4109	1.2688
	997.0	0.3910	1.1971
	1017.0	0.3717	1.1293
	1035.6	0.3576	1.0786
	1055.5	0.3453	1.0333
	1075.4	0.3292	0.9774
	1097.5	0.3151	0.9273
	1117.6	0.3038	0.8868
	1137.4	0.2942	0.8518
	1158.1	0.2843	0.8162
	1178.2	0.2756	0.7847
	1197.8	0.2668	0.7536

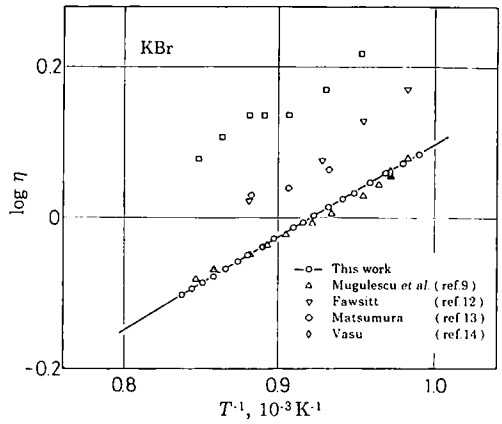

Fig. 6. Viscosity (in mPa·s) of molten potassium bromide.

Fig. 2b, the difference between the Δh's for both sample salt and water is less than 0.3 mm, which corresponds to about 0.4% of the effective height. Furthermore, they compensate each other to reduce the error.

(d) Corrosion of the capillary by molten salts: In this work, viscometer constants are checked before and after the measurement. The difference between them is 0.1–0.4%. This value is comparable to the uncertainty in the calibration, about 0.2–0.3%, and no devitrification of the capillary after the measurement is found by visual observation. Based on the above examination, the total error in the measurement is considerably small, probably less than 0.7%.

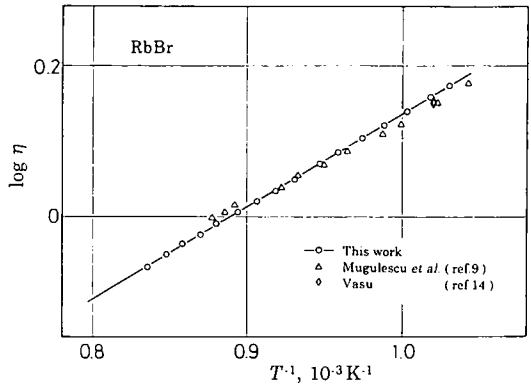

Fig. 7. Viscosity (in mPa·s) of molten rubidium bromide.

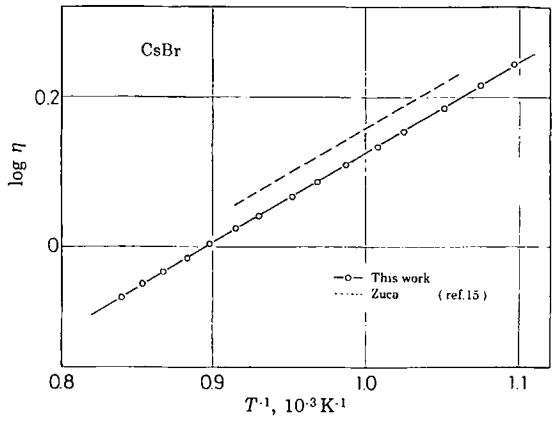

Fig. 8. Viscosity (in mPa · s) of molten cesium bromide.

To discuss the behavior of the viscosity on the alkali–metal halides, plots of $\log \eta$ vs. $1/T$ for all the alkali–metal halides are shown in Fig. 14. The symbols indicating alkali species indicate the temperature range of measurements for each salt. The viscosities of alkali–metal fluorides and chlorides are taken from the data which were also measured by one of the present authors (Y.S.) using an oscillating viscometer for fluorides [17] and the capillary viscometer for chlorides [18], respectively. No clear systematic variation in viscosity with the atomic number of the alkali–metal cation and halide anion is found, and all the salts except fluorides show similar viscosities in spite of large differences in ionic radius or ionic

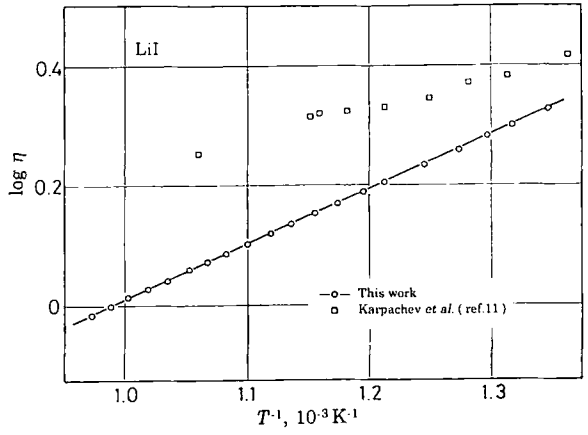

Fig. 9. Viscosity (in mPa · s) of molten lithium iodide.

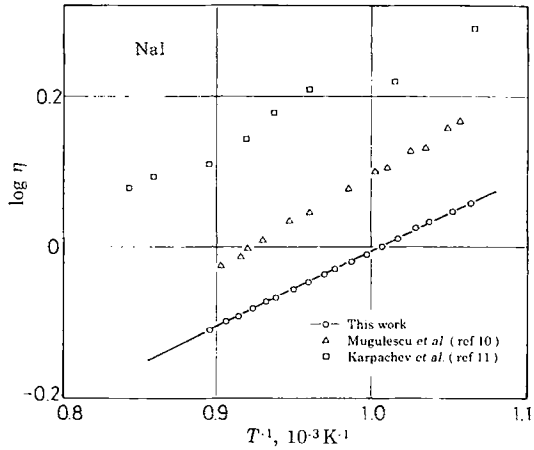

Fig. 10. Viscosity (in mPa·s) of molten sodium iodide.

weight among the salts. Therefore, the melting temperatures are taken as a parameter of the energy term of the melts. Figure 15 shows the relationship between the melting temperature and the apparent activation energy of viscous flow for all the melts. A significant correlation is found between them except for rubidium and cesium halides, which show higher apparent activation energies. The two lines with the correlation coefficients in Fig. 15 indicate that the melting temperature almost becomes a good parameter of the activation energy of viscous flow for alkali–metal halides except rubidium and cesium halides.

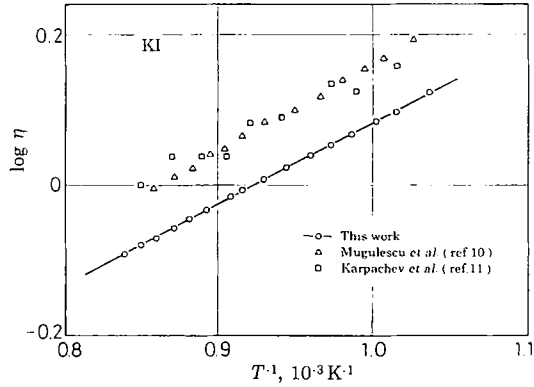

Fig. 11. Viscosity (in mPa·s) of molten potassium iodide.

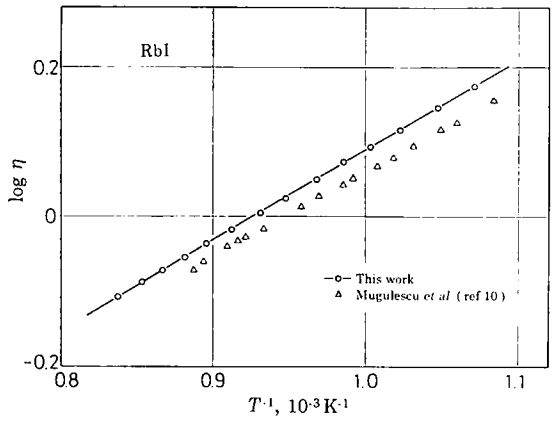

Fig. 12. Viscosity (in mPa · s) of molten rubidium iodide.

Hard sphere approximation is considered to be effective for alkali–metal halide melts since the melts consist of simple ions as mentioned above. Dymond [19] expressed the viscosity as a function of the volume and the temperature, and van Loef [20] gave the hard sphere volume V_0 by plotting $T^{1/2}/\eta$ vs. the molar volume of the melt. The relationship between them is expressed by Eq. (3), where A is a constant and depends on the salt.

$$T^{1/2}/\eta = A V_0^{1/3}(V_m - 1.384 V_0) \tag{3}$$

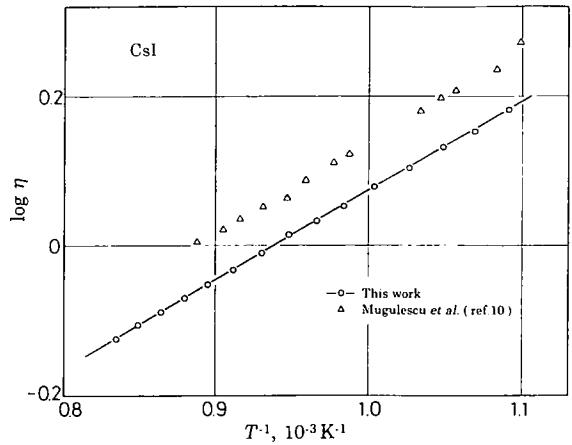

Fig. 13. Viscosity (in mPa · s) of molten cesium iodide.

Table II. Equations for Viscosities of Molten Alkali-Metal Bromides and Iodides

Salt	η (mPa·s)	SD (mPa·s)	Temp. range (K)
LiBr	0.14025·exp(17,249/RT)	0.0029	823–1082
NaBr	0.10334·exp(20,481/RT)	0.0020	1022–1193
KBr	0.07367·exp(23,548/RT)	0.0012	1010–1194
RbBr	0.08061·exp(23,549/RT)	0.0020	971–1197
CsBr	0.08470·exp(22,919/RT)	0.0031	911–1192
LiI	0.12647·exp(17,386/RT)	0.0018	742–1029
NaI	0.09938·exp(19,099/RT)	0.0030	940–1117
KI	0.10226·exp(20,523/RT)	0.0029	965–1193
RbI	0.07634·exp(23,083/RT)	0.0023	933–1194
CsI	0.07725·exp(22,698/RT)	0.0026	916–1198

The hard sphere radius, r_{HS}, and packing fraction, μ, in the melt are given by Eqs. (4) and (5) by assuming the fcc as a structure of close-packed spheres.

$$r_{HS} = (\sqrt{2}\, V_0/N)^{1/3}/2 \tag{4}$$

$$\mu = 4\pi r_{HS}^3 N/3V_m \tag{5}$$

where N and V_m are Avogadro's number and the molar volume of the melt. The ratio of r_{HS} to $(r_c^3 + r_a^3)^{1/3}$, where r_c and r_a are the anionic and cationic

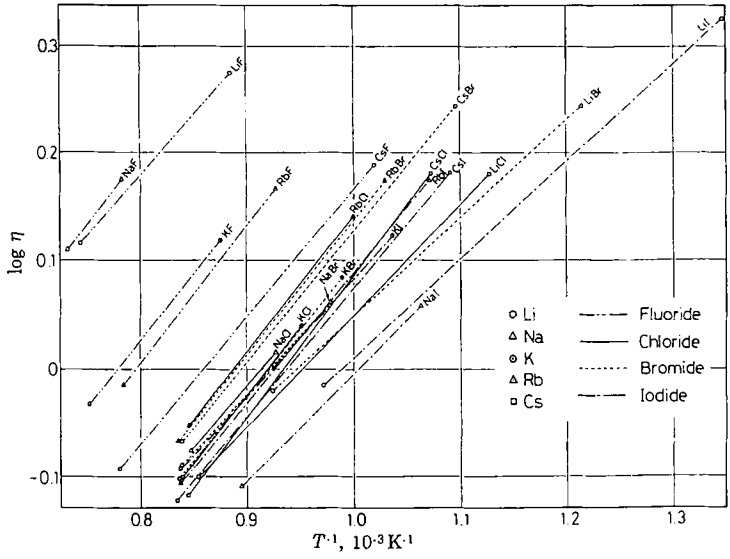

Fig. 14. Viscosities of all the molten alkali-metal halides.

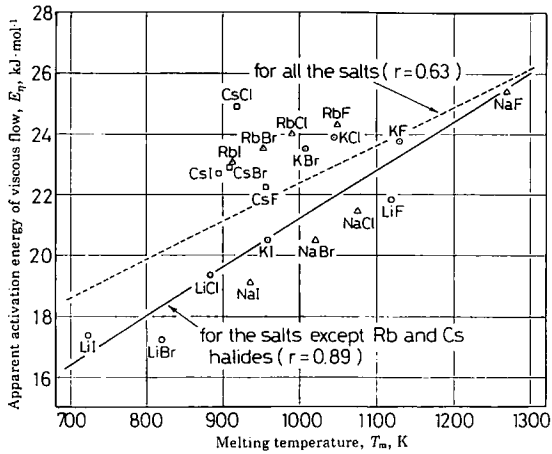

Fig. 15. The apparent activation energy of viscous flow of all the alkali-metal halides plotted against their melting temperatures. The dashed line indicates the correlation for all the salts, and the solid line indicates that for the salts except rubidium and cesium halides with correlation coefficients, respectively.

radii, using Pauling's ionic radii, is calculated for evaluating r_{HS}. Density data, which are needed in addition to viscosity for calculating the above values, of fluorides and chlorides are taken from the authors' previous data [21–23] for NaF, LiCl, NaCl, and CsCl, Yaffe's data [8, 24] for LiF, KF, CsF, KCl, and RbCl, and Jaeger's data [25] for RbF. The above values calculated are given in Table III. The ratios $r_{HS}/(r_c^3+r_a^3)^{1/3}$ are almost-unity. It is suggested that the flow unit for viscous flow of the alkali–metal halide melt is the cation–anion pair. This is reasonable because the distance between different-sign ions decreases and that between same-sign ions increases [26], therefore a cation probably makes the bond with the specified anion semipermanently. Small values of the ratio for lithium halide may be due to the polarization of the anion [7] by the strong electric field of lithium cation, which causes the effective radius of the hard sphere to decrease. In a transport process such as viscous flow, a flow unit, which is probably an ion pair in this case, jumps to a stable position from another position. It is important to estimate the volume of the hole or void which accepts the flow unit for considering the mechanism of viscous flow. Fürth [27] expressed the hole volume, v_h by using the surface tension of the liquid as shown below.

$$v_h = 0.68(kT/\gamma)^{3/2} \tag{6}$$

Table III. Hard-Sphere Volume V_0, Ratio of the Hard Sphere Radius to the Radius of the Cation-Anion Pair $r_{HS}/(r_c^3+r_a^3)^{1/3}$, Packing Fraction μ, and Hole Volume V_h at Melting Temperature

Salt	V_0 (10^{-6} m^3·mol^{-1})	μ	$r_{HS}/(r_c^3+r_a^3)^{1/3}$	V_h (10^{-30} m^3)
LiF	9.3	0.45	1.00	
NaF	13.4	0.46	1.05	
KF	19.2	0.47	1.05	
RbF	23.1	0.48	1.06	
CsF	27.1	0.48	1.03	
LiCl	18.8	0.44	0.97	20.5
NaCl	23.6	0.45	1.01	32.1
KCl	31.1	0.47	1.03	38.5
RbCl	34.7	0.48	1.04	37.9
CsCl	40.1	0.49	1.03	37.3
LiBr	23.2	0.44	0.96	22.7
NaBr	28.0	0.45	1.00	35.7
KBr	35.9	0.47	1.03	41.5
RbBr	39.6	0.48	1.03	40.0
CsBr	44.6	0.49	1.02	40.8
LiI	29.3	0.43	0.94	23.4
NaI	35.3	0.45	0.98	39.6
KI	43.3	0.46	1.01	47.2
RbI	48.0	0.48	1.02	45.5
CsI	54.2	0.49	1.02	48.4

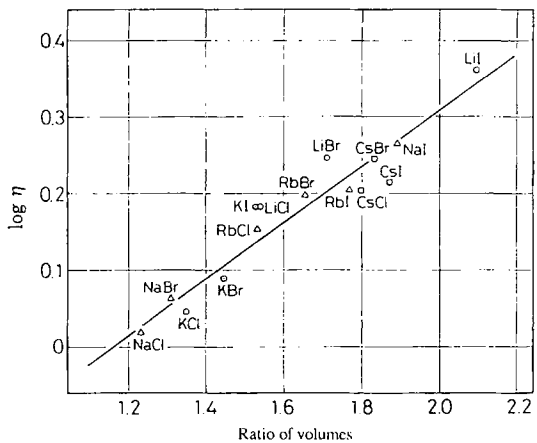

Fig. 16. Relationship between the logarithm of viscosity and the ratio of hard sphere volume to hole volume for chlorides, bromides, and iodides at their melting temperatures.

Since surface tension data on alkali–metal fluorides in the literature are not necessarily reliable, calculation is carried out for chlorides, bromides, and iodides whose surface tensions have been measured systematically by the present authors [7]. The relationship between the logarithmic viscosity and the ratio $V_0/v_h N$ is shown in Fig. 16, and a good correlation is found. This means that the viscous movement of the flow unit becomes more difficult when the size of the flow unit is larger than the size of hole. This is an effective assumption although the mechanism of viscous flow of the ionic melt is considered to be complex and Fürth's equation is somewhat doubtful as to whether surface tension as a macroscopic property is applicable to a microscopic pore of the atomic level.

4. CONCLUSION

Viscosities of all the alkali–metal bromide and iodide melts were measured precisely using a newly developed capillary viscometer made of quartz combined with a transparent electric furnace up to about 1200 K. The salt can be sealed in the viscometer under vacuum and the meniscus of the liquid is detected visually. A suspended liquid level-type outlet was employed to feed an arbitrary amount of liquid and to deal with the volume change of the liquid, and a downward funnel was built at the end of capillary in order to minimize the effect of the surface tension of the liquid. The reproducibility of measurements is less than 0.1% and the total error estimated is less than 0.7%.

The viscosity behavior of all the alkali–metal halides was studied. The apparent activation energy of viscous flow increases with an increase in melting temperature of the alkali–metal halide. A hard sphere approximation was adopted to evaluate the viscosity. A linear relation was found between the logarithmic viscosity and the ratio of hard sphere volume and hole volume at melting temperatures of alkali–metal halides.

ACKNOWLEDGMENT

The authors would like to thank the glass blower, Mr. Kazuo Horasawa, Tohoku University, for his excellent skill in the very difficult construction of the quartz viscometer.

REFERENCES

1. L. Stachowicz and L. Suski, *Electrochim. Acta* **19**:787 (1974).
2. H. Bloom, B. S. Harrap, and E. Heymann, *Proc. Roy. Soc. London* **194A**:237 (1948).
3. R. E. Wellman, R. DeWitt, and R. B. Ellis, *J. Chem. Phys.* **44**:3070 (1966).

4. J. D. Kellner, *J. Phys. Chem.* **71**:3254 (1967).
5. N. van Os and J. A. A. Ketelaar, *J. Electrochem. Soc.* **123**:1359 (1976).
6. G. G. W. Greening and K. G. Weil, *Z. Naturforsch.* **42a**:1283 (1987).
7. Y. Sato, T. Ejima, M. Fukasawa, and K. Abe, *J. Phys. Chem.* **94**:1991 (1990).
8. I. S. Yaffe and E. R. van Artsdalen, *J. Phys. Chem.* **60**:1125 (1956).
9. I. G. Murgulescu and S. Zuca, *Z. Phys. Chim.* [*Leipzig*] **218**:379 (1961).
10. I. G. Murgulescu and S. Zuca, *Rev. Roumaine Chim.* **10**:123 (1965).
11. S. Karpachev and A. Stromberg, *Zh. Fiz. Khim.* **11**:852 (1938).
12. C. E. Fawsitt, *J. Chem. Soc.* **93**:1299 (1908).
13. Y. Matsumura, M. Mizuno, and K. Nishihara, *Trans. Min. Metal. Assoc. Kyoto* **16**:167 (1967).
14. G. Vasu, *Rev. Roumaine Chim.* **14**:167 (1969).
15. G. J. Janz, *J. Phys. Chem. Ref. Data* [cited from Ph.D. thesis of Zuca, S., Bucharest, Roumania] **6**:419 (1977).
16. G. Jones and R. E. Stauffer, *J. Am. Chem. Soc.* **59**:1630 (1937).
17. T. Ejima, Y. Sato, S. Yaegashi, T. Kijima, E. Takeuchi, and K. Tamai, *J. Jpn. Inst. Metals* **51**:328 (1987).
18. T. Ejima, K. Shimakage, Y. Sato, H. Okuda, N. Kumada, and A. Ishigaki, *J. Chem. Soc. Jpn.* **6**:961 (1982).
19. J. H. Dymond, *J. Chem. Phys.* **60**:969 (1976).
20. J. J. van Loef, *Z. Naturforsch.* **31a**:967 (1976).
21. Y. Sato, A. Kojima, and T. Ejima, *J. Jpn. Inst. Metals* **41**:1249 (1977).
22. Y. Sato, K. Kobayashi, and T. Ejima, *J. Jpn. Inst. Metals* **43**:97 (1979).
23. T. Ejima, Y. Sato, A. Ando, and T. Asakawa, *J. Jpn. Inst. Metals* **45**:368 (1981).
24. I. S. Yaffe and E. R. van Artsdalen, *ORNL*-2159 (1956), p. 77.
25. F. M. Jaeger, *Z. Anorg. Allgem. Chem.* **101**:1 (1917).
26. K. Furukawa, *Disc. Faraday Soc.* **32**:53 (1960).
27. R. Fürth, *Proc. Cambr. Phil. Soc.* **37**:252 (1941).